

# Optimal Aeroelastic Design of an Oblique Wing Structure

L. B. Gwin\*

NASA Ames Research Center, Moffett Field, Calif.

A procedure is presented for determining the optimal cover panel thickness of a wing structure to meet specified strength and static aeroelastic divergence requirements for minimum weight. Efficient reanalysis techniques using discrete structural and aerodynamic methods are used in conjunction with resizing algorithms driven by optimality criteria. The optimality conditions for the divergence constraint are established and expressions are obtained for derivatives of the dynamic pressure at divergence with respect to design variables. The procedure is applied to an oblique wing aircraft where strength and stiffness are critical design considerations for sizing the cover thickness of the wing structure.

## Nomenclature

- $[A]$  = adjoint matrix for divergence eigenvalue problem
- $a_i$  = specified lower bounds on variable size
- $c_i$  = weight constants
- $C_{l\alpha i}$  = sectional lift-curve slope at station  $i$
- $[E_a]$  = aerodynamic induction or downwash matrix
- $[E_s]$  = flexibility influence coefficient matrix
- $(EI)_i$  = bending stiffness parameter at station  $i$
- $(GJ)_i$  = torsional stiffness parameter at station  $i$
- $h_i$  = depth of wing structural box at station  $i$
- $I_i$  = moment of inertia at station  $i$
- $J_s$  = set of design variables governed by side constraints
- $J_b$  = set of design variables governed by behavioral constraints
- $k$  = design iteration index
- $\{\ell\}$  = lift per unit span
- $M_i$  = bending moment at station  $i$  due to applied loading
- $n$  = number of design variables
- $q$  = eigenvalue representing dynamic pressure
- $q_D$  = dynamic pressure at divergence
- $q_{DS}$  = specified dynamic pressure at divergence
- $\{r\}$  = adjoint eigenvector for divergence eigenvalue problem
- $\{t\}$  = design variable vector
- $t_i$  = design variable at station  $i$
- $\Delta t_i$  = incremental change in variable  $t_i$
- $W$  = structural weight function
- $w_i$  = chordwise width of wing structural box at station  $i$
- $y_i$  = maximum distance from neutral axis of wing structural box
- $\alpha$  = relaxation factor
- $\beta_i$  = resizing parameter
- $\{\alpha\}$  = angle of attack vector
- $\lambda$  = multiplier in optimality criterion
- $\sigma_i$  = computed bending stress in  $i$ th member.
- $\bar{\sigma}_i$  = allowable bending stress in  $i$ th member

## I. Introduction

THE National Aeronautics and Space Administration is currently conducting feasibility studies of a transport aircraft with a pivoted, continuous wing that can be rotated from a conventional position at takeoff and landing to an

Presented as Paper 74-349 at the AIAA/ASME/SAE 15th Structures, Structural Dynamics and Materials Conference, Las Vegas, Nev., April 17-19, 1974; submitted May 6, 1974; revision received Feb. 18, 1975. This research was supported by National Research Council and NASA Ames Research Center, Advanced Vehicle Concepts Branch.

Index categories: Aeroelasticity and Hydroelasticity; Structural Design, Optimal.

\*NRC Research Associate. Member AIAA.

oblique angle at cruise conditions (Fig. 1). An oblique wing aircraft has been shown to create significantly smaller wave drag than symmetric configurations.<sup>1</sup> It can be operated economically at Mach 1.2 without a sonic boom and can takeoff and land at lower speeds with less noise than previously considered supersonic transport concepts. The pivot structure of such a design is also a more simple mechanism than the variable-sweep wing apparatus in use on current military airplanes and avoids the high bending moments associated with transmitting loads at the pivot itself.

However, swept forward wings are known to exhibit lower aeroelastic divergence speeds than straight or swept back wings, and preliminary investigation of the oblique wing concept<sup>2</sup> indicates that the design of the wing structure is governed by stiffness requirements as well as strength requirements.

This paper presents a method of determining the optimal panel thickness distribution of wing structure so that the material weight is minimized subject to a specified acceptable static divergence speed and to strength limitations for an assumed critical loading. This is accomplished by applying the conditions for optimality in an iterative procedure that minimizes structural weight, with constraints imposed on the dynamic pressure at divergence, member stresses, and lower bounds on panel thickness. If a fixed external configuration is assumed for aerodynamic considerations, the optimal stiffness and strength distributions are found, using design variables that size the cover panels.

Analysis and optimization methods have been selected for their efficiency during the redesign process. In contrast to half-model analysis of conventional symmetric configurations, flow over the entire wing is considered. The specific optimality criterion for static aeroelastic divergence is presented in detail. It is derived by using the generalized method outlined in a recent report by Kiusalaas.<sup>7</sup> It is driven by a resizing procedure known to be effective for optimality criteria. Analytic gradient expressions developed to drive the aeroelastically constrained problem are discussed in the following section.

## II. Optimal Design for Specified Divergence Speed

The equilibrium equations that express the static neutral stability of the elastic wing structure are written in matrix form as

$$[E_a] \{\ell\} = q [E_s] \{\ell\} \quad (1)$$

where  $[E_a]$  = aerodynamic induction or downwash matrix,  $[E_s]$  = flexibility influence coefficient matrix,  $\{\ell\}$  = lift per unit span, and  $q$  = dynamic pressure.

Equation (1) indicates a balance of displacements due to aerodynamic loading and elastic restoring forces when

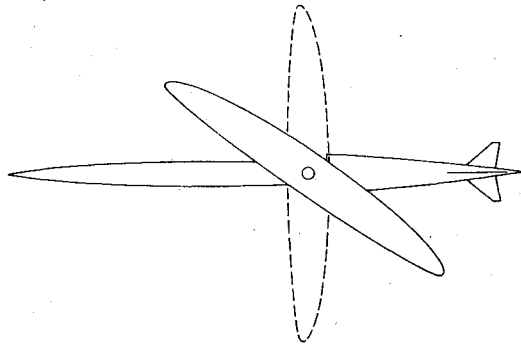


Fig. 1 Oblique wing transport aircraft.

dynamic motion can be neglected. The aeroelastic divergence of the oblique wing transport as the solution to the corresponding dynamic equations of motion was discussed recently by Jones and Nisbet.<sup>3</sup>

At speeds above a critical value associated with the dynamic pressure at divergence  $q_D$ , the aerodynamic forces of Eq. (1) will overcome the elastic restoring forces and instability will occur if the wing is restrained in roll. To assure stability, a 20% margin over the design speed of the aircraft is required, which dictates the constraint for stiffness design of the oblique wing structure. Wind-tunnel<sup>4</sup> and analytical results at Ames Research Center indicate such wings may be flutter critical in a symmetric position at lower speeds.

The least weight structure that satisfies the divergence requirement is found by applying the criterion for optimality to the reduction of a function that represents the weight of the members

$$W(\{t\}) = \sum_{i=1}^n c_i t_i \quad (2)$$

as a linear combination of  $n$  design variables  $t_i$  with the constraint on divergence

$$q_D \geq q_{DS} \quad (3)$$

and  $n$  side constraints on variable lower bounds

$$t_i \geq a_i \quad i = 1, 2, \dots, n \quad (4)$$

where the  $c_i$ ,  $q_{DS}$ , and  $a_i$  are specified constants.

#### Structural Model

The high aspect ratio of the wing implies that the structure can be reasonably modeled as a beam. Consequently, the spanwise variation in section is approximated by beam elements at discrete points along the wing.

The flexibility influence coefficient matrix of Eq. (1) is based on the relationship

$$[E_s] \{\ell\} = \{\alpha\} \quad (5)$$

where  $\alpha_i$  is the local streamwise angle of attack. The influence coefficients themselves are derived from the transformation of local pitching and rolling moments from the lift at quarter-chord into beam bending and torsional moments about the elastic axis.<sup>5</sup> Values of bending and torsional stiffness are considered to be constant over each spanwise increment. Each matrix element  $E_{sij}$  represents the angle of attack (in radians) at station  $i$  caused by structural deformation from unit loading at station  $j$ .

The material of each section is considered concentrated entirely in the upper and lower cover sheets, so that the bending and torsional stiffnesses can be approximated by

$$(EI)_i = (E_i w_i h_i^2 / 2) t_i \quad (6)$$

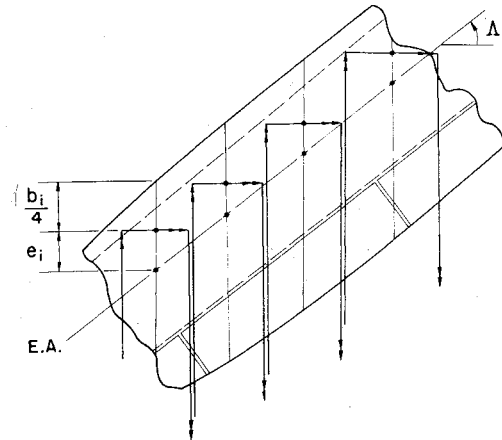


Fig. 2 Planform section.

$$(GJ)_i = 0.8 (EI)_i \quad (7)$$

Local thickness  $t_i$  is permitted to vary during redesign, and depth  $h_i$ , width  $w_i$ , and modulus  $E_i$  are considered constant.

The beam was assumed fixed at the pivot attachment to the fuselage. This restriction restrains the vehicle in roll – an important consideration in balancing aerodynamic loads with the wing in an oblique position.<sup>6</sup> (More complete calculations show that the speed at which aeroelastic instability occurs in flight is higher than that calculated if the fuselage is assumed to be restrained in roll. However, in all cases investigated thus far, the static divergence that appears when the fuselage is clamped provides a conservative estimate of the actual stability in free flight, i.e., a lower  $q_D$ .)

#### Aerodynamic Model

As a first approximation to the spanwise lift distribution, an element lifting line theory<sup>5</sup> was used in conjunction with the beam structural model. Figure 2 shows a system of constant strength horseshoe vortices that produce concentrated lift loads at the element quarter-chord point a distance  $e_i$  ahead of the beam structural node located on the elastic axis.

The aerodynamic induction matrix of Eq. (1) is related to the angle-of-attack vector by

$$(1/q) [E_a] \{\ell\} = \{\alpha\} \quad (8)$$

where

$$[E_a] = \left[ \frac{1}{C_{l\alpha i}} \right] [\bar{E}_a] \quad (9)$$

so that the effect of local values of the sectional life-curve slope  $C_{l\alpha i}$  is a weighting influence on the system. The coefficients  $E_{aij}$  in Eq. (8) express proportionality between the downwash angle at a control point at station  $i$  and the lift per unit dynamic pressure at station  $j$ . They are computed on the assumption that the downwash angle at the control point, located at three-quarter chord, will equal the geometric angle of attack. The method of computing coefficients over the entire span of the wing was modified from that in Ref. 5 to remove symmetry restrictions.

#### Constraint Evaluation

Each new move in the design space during the optimization process requires evaluation of the proximity of the new design to the constraint boundaries. The side constraints of Eq. (4) are easily checked by comparing each variable with its lower bound, but the divergence constraint of Eq. (3) requires determination of  $q_D$  at the design point in question.

The dynamic pressure at divergence is identified as the lowest eigenvalue of the eigensystem represented by Eq. (1).

Because only the lowest eigenvalue is required, matrix iteration by the power method can be applied to the system

$$(1/q)\{\ell\} = [E_a]^{-1}[E_s]\{\ell\} \quad (10)$$

And since for steady flow the aerodynamic matrix is independent of changes in the design, its inverse can be precomputed outside the design loop.

Evaluating the divergence constraint thus requires that the structural matrix be updated to reflect the current design by use of Eqs. (6) and (7), premultiplication of this matrix by the inverted aerodynamic matrix of Eq. (9), and solution of the eigensystem of Eq. (10). Updating the flexibility influence coefficients is computationally efficient because of the simplicity of the beam model, and convergence to  $q_D$  by iteration is usually rapid, especially when the eigenvector of the previous design has been saved for restarting.

#### Derivative Calculation

Derivatives that express the rate of change of the divergence eigenvalue  $q_D$  with respect to design variables  $t_i$  can be derived by considering Eq. (1) in the form

$$[A]\{\ell\} = \{0\} \quad (11)$$

with

$$[A] \equiv [E_a] - q[E_s] \quad (12)$$

The adjoint problem is then

$$[A]^T\{r\} = \{0\} \quad (13)$$

which implies

$$\{r\}^T[A] = \{0\}^T \quad (14)$$

Differentiating Eq. (11) with respect to variable  $t_i$  gives

$$\left(0 - \frac{\partial q}{\partial t_i}[E_s] - q \frac{\partial}{\partial t_i}[E_s]\right)\{\ell\} + [A] \frac{\partial}{\partial t_i}\{\ell\} = \{0\} \quad (15)$$

where the first term vanishes from the invariance of the aerodynamic matrix with respect to the selected design parameters.

Premultiplying Eq. (15) by the transpose of the adjoint eigenvector and utilizing Eq. (14) produces the following scalar equation

$$\{r\}^T \left( - \frac{\partial q}{\partial t_i}[E_s] - q \frac{\partial}{\partial t_i}[E_s] \right) \{\ell\} + 0 = 0 \quad (16)$$

Equation (16) can then be solved for the derivative of the dynamic pressure

$$\frac{\partial q}{\partial t_i} = -q \frac{\{r\}^T \frac{\partial}{\partial t_i}[E_s]\{\ell\}}{\{r\}^T[E_s]\{\ell\}} \quad (17)$$

When this quantity is computed at a particular design point using the  $q_D$  obtained from the constraint evaluation of Eq. (10) and the corresponding eigenvectors of the regular and adjoint problems, the divergence gradient can be formed as

$$\{\nabla q_D\}^T = \left( \frac{\partial q_D}{\partial t_1} \frac{\partial q_D}{\partial t_2} \dots \frac{\partial q_D}{\partial t_n} \right) \quad (18)$$

Derivatives of the structural influence coefficient matrix in the numerator of Eq. (17) are computed by examining the

contributions of the element stiffness of Eqs. (6) and (7) to the generation of the structural matrix. These derivative matrices are constant and need not be computed within the design loop.

#### Optimization Procedure

Kiusalaas<sup>7</sup> has outlined a systematic procedure for optimal structural design using a gradient-based optimality criterion algorithm for resizing. It is adapted here to the divergence constrained problem.

If a linearization of the expression for incremental change in  $q_D$  is assumed

$$\Delta q_D \approx \sum_{i=1}^n \frac{\partial q_D}{\partial t_i} \Delta t_i \quad (19)$$

then conditions can be developed for design changes that will simultaneously reduce the weight and maintain  $\Delta q_D = 0$ . Note that this strategy represents limitation to a small region near the behavioral constraint hypersurface, so that it effectively becomes a condition for local optimality.

The criterion for an optimal design to exist can be shown to be

$$c_i - \lambda \frac{\partial q_D}{\partial t_i} = 0 \quad \text{if } a_i < t_i \quad (20a)$$

$$c_i - \lambda \frac{\partial q_D}{\partial t_i} \geq 0 \quad \text{if } a_i = t_i \quad (20b)$$

where the  $c_i$ 's are the weight constants of Eq. (2) and the  $a_i$ 's are the specified lower bounds on variable size from Eq. (4).

The multiplier is computed as

$$\lambda = \frac{q_{DS} - q_D + \sum_{j \in J_s} \frac{\partial q_D}{\partial t_j} (t_j - a_j) + (1 - \bar{\alpha}) \sum_{j \in J_b} \frac{\partial q_D}{\partial t_j} t_j}{(1 - \bar{\alpha}) \sum_{j \in J_b} \left( \frac{\partial q_D}{\partial t_j} \right) \frac{t_j}{c_j}} \quad (21)$$

Parameter  $\bar{\alpha}$  is a relaxation factor that determines the rate of convergence. Most applications require that

$$0 < \bar{\alpha} < 1 \quad (22)$$

The  $J_s$  and  $J_b$  are those sets of variables classified as being currently governed by the side constraints or behavioral constraint, respectively. Figure 3 indicates a redesign procedure that utilizes the classification of variables as belonging either to set  $J_s$  or  $J_b$ . This process uses the criterion of Eq. (20) in the following resizing formula:

$$t_i^{(k+1)} = \beta_i t_i^{(k)} \quad \text{if } \beta_i t_i^{(k)} \geq a_i \quad (23a)$$

$$t_i^{(k+1)} = a_i \quad \text{if } \beta_i t_i^{(k)} < a_i \quad (23b)$$

where the scale factor  $\beta_i$  is defined as

$$\beta_i \equiv \bar{\alpha} + (1 - \bar{\alpha}) \frac{\lambda}{c_i} \frac{\partial q_D}{\partial t_i} \quad (24)$$

The initial design of Fig. 3 is analyzed and the behavioral constraint and side constraints of Eqs. (3) and (4) are evaluated. If the design is outside a specified tolerance band about the behavioral constraint, a behavioral modification cycle is entered which drives the design along the divergence gradient until capture is achieved.

The gradient vector of Eq. (18) is then computed and tested. Negative elements of this vector imply that the associated design variable, in the neighborhood of the optimum, can produce a lighter weight by decreasing as much as possible. Such variables are thus classified as belonging to set  $J_s$ . All

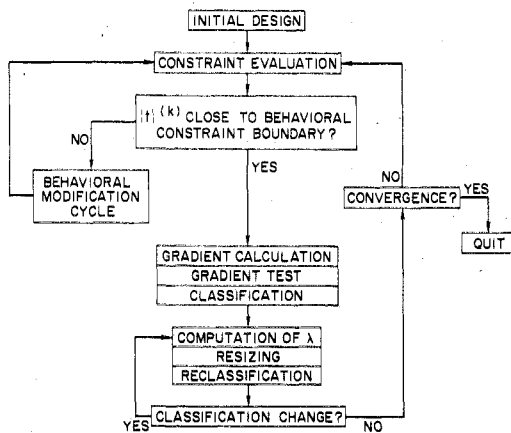


Fig. 3 Optimizing flow diagram.

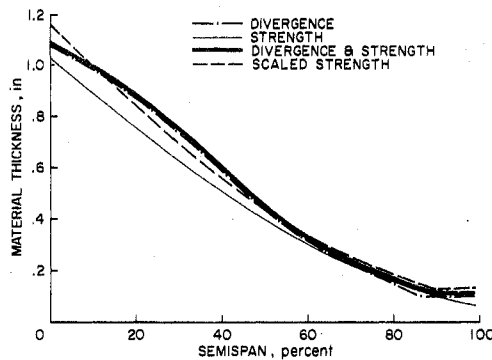


Fig. 4 Optimal thickness distributions.

others are capable of weight reduction by moves along the behavioral constraint and are grouped as  $J_b$ .

The multiplier of Eq. (21) and scale factors of Eq. (24) are computed and the variables are resized according to Eq. (23). Any variables that can be reduced to their lower bounds are reclassified as belonging to  $J_s$ , and the scaled variables to  $J_b$ . This cycle is repeated until no further change in reclassification occurs. When the system has converged to a stable value of the structural weight, the procedure is discontinued. Otherwise, constraints for the new design are evaluated and the entire process is repeated.

### III. Optimal Design for Strength

For preliminary sizing of the cover-sheet thickness necessary to satisfy strength requirements, a single loading condition may be used that represents the most severe combination of applied loads the structure must withstand throughout the flight envelope. For one set of loads, a structure with fixed external geometry and specified materials will usually converge to a fully stressed design<sup>8</sup> by repeated application of a stress ratio algorithm

$$t_i^{(k+1)} = t_i^{(k)} (\sigma_i^{(k)} / \bar{\sigma}_i) \quad (25)$$

where  $\sigma_i^{(k)}$  = computed stress in  $i$ th member for  $k$ th design, and  $\bar{\sigma}_i$  = corresponding allowable stress for that member.

It is well known that such a process will converge in one step if the structure is statically determinant. For this special case, the design can also be shown to be optimal, i.e., minimum weight, even though there is no attempt to minimize an objective function.

Since the beam model used in this investigation meets these requirements, the optimal strength design can be computed directly from Eq. (25). When the cover design is governed by

the bending stress, Eqs. (6) and (25) establish that

$$t_i^{(k+1)} = \frac{t_i^{(k)}}{\bar{\sigma}_i} \frac{M_i y_i}{I_i} \quad (26a)$$

$$t_i^{(k+1)} = \frac{t_i^{(k)}}{\bar{\sigma}_i} \left( \frac{M_i h_i / 2}{t_i^{(k)} w_i h_i^2 / 2} \right) \quad (26b)$$

$$t_i^{(k+1)} = \frac{M_i}{\bar{\sigma}_i w_i h_i} \quad (26c)$$

where  $M_i$  is the local bending moment due to applied loading. It is assumed that such moments are not functions of the design and that the applied loading is symmetric over the span.

Further, Eq. (26) implies that each of the strength constraints for optimization are functions of a single variable since the inequalities

$$\sigma_i \leq \bar{\sigma}_i \quad (27)$$

can be written as

$$M_i / \bar{\sigma}_i w_i h_i \leq t_i \quad (28)$$

which has the same form as inequality (4).

### IV. Optimal Design for Strength and Divergence

For applications where the wing structure can be modeled as a statically determinate beam, the combined strength and divergence constrained problem can, therefore, be solved using the method of Sec. II, with the lower bounds specified as either the strength restrictions of inequality (28) or as minimum gage from inequality (4), whichever is higher.

### V. Application to Oblique Wing Structure

The method was applied to the least-weight design of an aluminum oblique wing structure with an aerodynamic planform represented by an 8:1 ellipse and thickness/chord ratio of 12% at the pivot. The spanwise depth distribution of the primary structure was elliptic, due to the specification of constant thickness/chord ratio.

The analysis model consisted of 20 spanwise beam elements with complete restraint at the pivot node. The depth, chord, span, and material properties were assumed constant for each element, with the design variable sizing the thickness of both the upper and lower panels. A balanced structure was assumed, so that 10 design variables designed both the forward and aft swept portions of the wing.

The strength design was based on the bending moment envelope resulting from a 3.37-g gust loading and symmetric 2.5-g maneuver loading as per Ref. 2. The allowable bending stress of Eq. (26) was taken as 63 ksi. Optimization for divergence was based on a sweep angle of 45 deg and a constant spanwise lift-curve slope of  $2\pi$  for Eq. (9). The specified divergence pressure  $q_{DS}$  was selected to produce a weight penalty of approximately 10% for the increased stiffness material for divergence, in accordance with the weight penalty observed for this configuration.<sup>2</sup> The relaxation factor in Eq. (21) was taken as 0.35, with a tolerance specification that the behavioral constraint evaluation be less than 0.3 to avoid initiation of the behavior modification cycle.

Figure 4 shows the optimal thickness distributions obtained by optimizing the structure for strength alone (thin solid curve) and for divergence alone (dash-dot curve). The strength design is fully stressed in the absence of the side constraints. However, design for divergence required the specification of minimum gage constraints (taken as 0.10 in.). The need for this specification is typical of the purely aeroelastically constrained problem.<sup>9</sup>

**Table 1 Weight comparison (lb)**

Strength	62,155
Divergence	69,471
Divergence and strength	69,568
Scaled strength	69,681

**Table 2 Computational times for combined design**

Time/iteration	Iterations	Time	Module
7.219	1	7.219	Behavior modification cycle
1.453	9	13.077	Constraint evaluation
1.951	9	17.559	Derivative calculation
0.015	11	0.165	Resizing cycle
		38.020	Total

The heavy solid curve of Fig. 4 is the divergence and strength design computed by the method of Sec. II, i.e., the optimal material distribution considering divergence, strength, and minimum gage constraints simultaneously. This design is nearly identical with the divergence design up to approximately 65% semispan and is identical with the strength and minimum gage design out to the tip. The dashed curve is the thickness distribution obtained by uniformly scaling up to the strength design (thin solid line) until the divergence and minimum gage constraints are satisfied. Note that all horizontal lines near the tip in Fig. 4 are meant to imply the identical value (0.10-in. minimum gage) but have been drawn slightly separated for visual clarification. Table 1 compares the weight of this design with the other designs in Fig. 4 in pounds of bending material for the primary wing structure.

## VI. Observations and Comments

The heavy solid and dashed curves in Fig. 4 each represent designs that satisfy the strength, divergence, and minimum gage requirements. The optimized design, however, is minimum weight. The small difference in weight indicates that, for this particular example, the design space in the neighborhood of this optimum is very flat. This means that relatively large variations in the optimal thickness distribution are possible at about the same weight. This feature is usually considered attractive for practical design considerations.

Table 1 also shows the weight savings if the structure were to be constructed without the restriction of spanwise symmetry in the thickness distribution. Because the sweptback wing would not be governed by divergence, the optimal design would be the fully stressed strength design (ignoring flutter requirements). The weight of a strength-designed aft wing with a forward wing designed for divergence and strength would be 5.3% lighter than that for which the divergence and strength design is imposed both forward and aft. However, there are disadvantages to manufacturing such a structure.

Each of the above designs was started from the stress ratio design and required only one behavior modification cycle to

bring the design sufficiently near the divergence constraint boundary where the linearized redesign algorithm was valid. From this point, rapid convergence was achieved along the boundary itself, nearly reaching the optimal design in only two or three iterations. Convergence was allowed only after successive iterations were within 1 lb.

Table 2 gives the time per iteration, the number of iterations, and the accumulated time spent in each of the four computational modules required to optimize the combined divergence, strength, and minimum gage design with 10 variables. These are approximate CPU seconds on an IBM 360/67 with FORTRAN G compilation in a time-sharing mode.

The method has been applied to a single design situation that exhibits an interaction between requirements for stiffness, strength, and minimum gage. Other combinations of planform configuration and material properties may lead to different results. For example, the same wing of graphite-epoxy honeycomb construction requires approximately the same amount of material for divergence and strength.<sup>2</sup> The method is apparently efficient for parametric studies at other flight conditions and for less simplistic stress and load analysis. Additional applications with more design parameters are expected to provide better assessment of computational efficiency. Although the procedure was developed for a single behavioral constraint, it does not depend on the analysis model. Thus, a more detailed structural and aerodynamic analysis is possible in conjunction with this method of optimization.

## References

- <sup>1</sup>Jones, R. T., "Reduction of Wave Drag by Antisymmetric Arrangement of Wings and Bodies," *AIAA Journal*, Vol. 10, Feb. 1972, pp. 171-176.
- <sup>2</sup>Kulfan, R. M., Neumann, F. D., Nisbet, J. W., Mulally, A. R., Murakami, J. K., Noble, B. C., McBarron, J. P., Stalter, J. L., Gimmetad, D. W., and Sussman, M. B., "High Transonic Speed Transport Aircraft Study - Final Report," NASA CR-114658, Sept. 1973.
- <sup>3</sup>Jones, R. T. and Nisbet, J. W., "Transonic Transport Wings - Oblique or Swept?" *Aeronautics and Astronautics*, Vol. 12, Jan. 1974, pp. 40-47.
- <sup>4</sup>Graham, L. A., Jones, R. T., and Boltz, F. W., "An Experimental Investigation of Three Oblique-Wing and Body Combinations at Mach Numbers Between 0.60 and 1.40," NASA TM X-62256, April 1973.
- <sup>5</sup>Gray, W. L. and Schenk, K. M., "A Method for Calculating the Subsonic Steady-State Loading on an Airplane Wing of Arbitrary Planform and Stiffness," NACA TN 3030, Dec. 1953.
- <sup>6</sup>Weisshaar, T. A. and Ashley, H., "Static Aeroelasticity and the Flying Wing," *Journal of Aircraft*, Vol. 10, Oct. 1973, pp. 586-594.
- <sup>7</sup>Kiusalaas, J., "Minimum Weight Design of Structures via Optimality Criteria," NASA TN D-7115, Dec. 1972.
- <sup>8</sup>Gallagher, R. H. and Zienkiewicz, O. C., *Optimal Structural Design*, Wiley New York, 1973, pp. 19-31.
- <sup>9</sup>Ashley, H. and McIntosh, S. C., Jr., "Applications of Aeroelastic Constraints in Structural Optimization," *Proceedings of the 12th International Congress of Applied Mechanics*, Springer, Berlin, 1969, pp. 100-113.